iVES OENO One vine & wine

DOI: https://doi.org/10.20870/oeno-one.2024.58.1.7823

OPEN ACCESS

ORIGINAL RESEARCH ARTICLE

Cultivar-dependent grape berry dehydration in later ripening phases may be associated with energy regulation and ionic homeostasis

Yin Liu*[1,2,3,4], Stephen D. Tyerman[1,5], Leigh M. Schmidtke[1,2,3] and Suzy Y. Rogiers[1,6]

[1] Australian Research Council Training Centre for Innovative Wine Production, Urrbrae, SA 5064, Australia
[2] School of Agricultural, Environmental and Veterinary Sciences, Charles Sturt University, Wagga Wagga, NSW 2648, Australia
[3] Gulbali Institute, Charles Sturt University, Wagga Wagga, NSW 2648, Australia
[4] School of Science, Guangdong University of Petrochemical Technology, Guangdong 525000, China
[5] Department of Wine Science and Waite Research Institute, University of Adelaide, Urrbrae, SA 5064, Australia
[6] New South Wales Department of Primary Industries, Wollongbar, NSW 2477, Australia

ABSTRACT

Climate warming and drought may alter the progression of sugar accumulation in the grape berry and contribute to pre-harvest berry shrivel and cell vitality loss, which have been hypothesised to be associated with solute accumulation cessation and energy status in the berry. To explore the relationship between energy and cultivar-dependent berry cell death, we characterised the variations in pericarp constituents and energy status across five time points, five ripening phases and 3 cultivars with various levels of berry shrivel and cell death. Grape berries of Shiraz, Chardonnay and Flame Seedless at the Eichorn-Lorenz stages 33 to 39 were sampled at 5:00, 9:00, 13:00, 17:00 and 21:00 on each sampling day. These were analysed for water percentage, adenosine triphosphate (ATP), ethanol, sugar and L-malic acid, as well as elements with vascular mobility, including potassium (K) and sodium (Na). The accumulation of sugar and phloem mobile elements ceased in Shiraz and Chardonnay during the later ripening phase, while Flame Seedless did not undergo water loss or stop accumulating solutes in the pericarp. Shiraz berry ripening was distinguished by greater pericarp water loss, ATP reduction, increased ion disorder susceptibility as indicated by a lower K/Na ratio, and higher ethanol concentration in the later ripening phase. The Chardonnay pericarp contained the highest ATP concentration and K/Na ratio of the 3 cultivars. The Flame Seedless pericarp maintained a low but stable K/Na ratio throughout berry ripening. The berry ripening phase impacted on diurnal trends in pericarp water percentage and ATP concentration. The results indicate that energy regulation and ionic homeostasis may be associated with cultivar-dependent grape pericarp hydration, solute accumulation and energisation during berry ripening.

KEYWORDS: adenosine triphosphate, cell vitality, energy, grape berry dehydration, potassium, solute accumulation, *Vitis vinifera*

*correspondence:
yinliu0426@outlook.com

Associate editor:
José Manuel Moutinho Pereira

Received:
15 October 2023

Accepted:
16 January 2024

Published:
13 February 2024

This article is published under the **Creative Commons licence** (CC BY 4.0).

Use of all or part of the content of this article must mention the authors, the year of publication, the title, the name of the journal, the volume, the pages and the DOI in compliance with the information given above.

INTRODUCTION

Grape berries (*Vitis vinifera.* L) are good sinks for sugars, attracting animals and aiding in seed dispersal (Coombe, 1976; Rogiers *et al.*, 2006b). Climate warming is causing early grape berry maturation (Webb *et al.*, 2012; Cameron *et al.*, 2020) and greater evapotranspiration that exacerbates berry dehydration. The reduction in phloem flow into the berry (Rogiers *et al.*, 2006a; Carlomagno *et al.*, 2018), transpiration (Greer and Rogiers, 2009) and xylem backflow (Tilbrook and Tyerman, 2009), as well as mesocarp cell vitality decline (Tilbrook and Tyerman, 2008; Fuentes *et al.*, 2010; Bonada *et al.*, 2013a; Bonada *et al.*, 2013b) all contribute to late-ripening berry shrivel prior to harvest. As no signs of stress have been observed in grapevine with berries showing cell death (Tilbrook and Tyerman, 2008), late-ripening berry weight loss and mesocarp cell death have been considered to be the physiological manifestation of berry senescence. These physiological changes are particularly apparent in certain wine grape cultivars, such as Shiraz (Rogiers and Holzapfel, 2015), while table grape berries with thinner skin and firmer flesh are not so prone to shrinkage during this final phase of ripening (Tilbrook and Tyerman, 2008; Tilbrook and Tyerman, 2009). Mesocarp cell death has been found to occur in mid-ripening Chardonnay berries with total soluble solid (TSS) lower than 22 °Brix (Tilbrook and Tyerman, 2008), along with curtailed xylem flow following veraison (Tilbrook and Tyerman, 2009). Solute accumulation may be vulnerable to the energy status of cells within the berry, because solutes are transported by vital and energised cells. Investigating the regulation of energy for the accumulation of solutes within the berry pericarp could provide insights into berry dehydration and cell vitality during the later phases of ripening.

Altered vascular transport appears to contribute to berry dehydration (Rogiers *et al.*, 2006a; Tilbrook and Tyerman, 2009; Carlomagno *et al.*, 2018). Vascular unloading into the pericarp can be inferred from the accumulation of solutes with mobility in the xylem or phloem (Rogiers *et al.*, 2006b). The potassium (K) ion with phloem mobility assists in sugar accumulation (Coetzee *et al.*, 2017; Rogiers *et al.*, 2017; Coetzee *et al.*, 2019). Magnesium (Mg) and phosphorus (P) are phloem mobile and accumulate in post-veraison berries (Coombe, 1976; Rogiers *et al.*, 2006b). Calcium (Ca) is a xylem-mobile element and mainly accumulates in seeds during berry development (Rogiers *et al.*, 2006b). The sodium (Na) ion is mainly transferred into grape berries via the xylem (Maathuis, 2014). Xiao *et al.* (2021) found that the efficiency of vascular transport into berries is partly the result of the anatomical parameters of the vascular tissues located within the various berry compartments: the vascular anatomical structures did not vary according to seediness, indicating that berry shrivel or mesocarp cell death evident in Shiraz and Chardonnay were not associated with the presence of seeds. Other mechanisms, such as solute compartmentation and metabolism, may be responsible for cultivar variations in terms of berry hydration and solute accumulation.

The energy required for accumulating solutes in grape berries increases with ripening; phloem unloading switches from the symplastic to the apoplastic pathway at the onset of ripening (Zhang *et al.*, 2006), thereby increasing the requirement for energised membranes. Fuelled by adenosine triphosphate (ATP), the plasma membrane and tonoplast are mainly energised by the translocation of cytosolic H^+ to the apoplast and vacuoles. Mesocarp hypoxia and ethanol accumulation have been found to be promoted in Shiraz and Chardonnay berries during ripening (Xiao *et al.*, 2018b), suggesting that suppressed aerobic respiration and limited ATP availability may occur in the berries during the late-ripening phase. However, ATP content in ripening berries and the roles of ATP on ripening parameters are still mostly unclear.

The role of ATP in grape berries may be associated with light intensity, as suggested by light-dependent ion fluxes from the grape berry mesocarp, which may be the consequences of membrane voltage alteration via light-sensitive H^+-ATPase (Shabala and Wilson, 2001). Light fluctuation has been found to alter the net uptake of K^+ from grape mesocarp tissue and be correlated with H^+ and Ca^{2+} flux, confirming that ion transport within the grape mesocarp is altered by light intensity (Shabala and Wilson, 2001). Exposing Shiraz berries to light and wind with higher temperature accumulation has been shown to result in a lower mesocarp cell vitality in overripe berries than in shaded berries, and thus can promote berry dehydration (Clarke and Rogiers, 2019). Given that light and temperature oscillate across the diurnal cycle, ATP availability and solute transport into and within grape berries may vary between daytime and nighttime. The potential diurnal fluctuation of energy status and solute transport may contribute to berry hydration regulation and the progression of ripening.

We hypothesised that berry dehydration in the late phase of ripening is associated with changes in berry energy status and solute transport. We therefore characterised the developmental patterns of several pericarp parameters in three grape cultivars, Shiraz, Chardonnay and Flame Seedless, with either high, medium or low degrees of berry weight loss and mesocarp cell death. To investigate day to night transitions in berry energy status, we applied a diurnal sampling regime comprising five time points on each sampling date. Energy status was quantified in terms of ATP and ethanol. An assessment of solute content on a pericarp basis bypasses the fluctuations in concentration that can result from changes in berry water status. The dynamics of five inorganic elements, namely phloem-mobile K, Mg and P, and xylem-mobile Ca and Na, were characterised to represent vascular inflow at various maturity stages. The maturity and hydration of the berry pericarp were assessed in terms of fresh mass, water mass, dry mass, water percentage, TSS, total sugar and L-malic acid.

MATERIALS AND METHODS

1. Grape berry sampling, partitioning and processing

Sampling was carried out on two wine grape cultivars, Shiraz and Chardonnay, and one table grape cultivar, Flame seedless, grown in north-south oriented rows in a replicated cultivar block in the vineyard of Charles Sturt University, Wagga Wagga, Australia (latitude: 35.06 °S; longitude: 147.36 °E, elevation: 219 m). This replicated cultivar block contained ten cultivars. Each cultivar was replicated 6 times in panels consisting of 3 vines of the particular cultivar. Each of the 6 rows represented one replicate of ten cultivars. The vines were drip irrigated to maintain physiological functions of the vines without stress, and managed according to best practice in the Australian wine industry. No sign of water stress or physiological dysfunction was apparent in the vines during the growing season. Climate data in the 2019–2020 season grapevine growing season [Supplementary Information. Figure S1], recorded by the climate station Wagga Wagga Amo (Station Number: 072150, latitude: 35.16 °S, longitude: 147.46 °E, elevation: 212 m), were accessed using Climate Data Online, Bureau of Meteorology (http://www.bom.gov.au/climate/data). The straight-line distance between the experimental site and the climate station is 13.8 km. Growing degree days (GDD) units were calculated using a baseline temperature of 10 °C from September 2019 (Jarvis *et al.*, 2017).

Three replicated panels, serving as three biological replicates, for Shiraz, Chardonnay and Flame Seedless were chosen for this study. Berry samples were collected at five ripening phases during the 2019–2020 vintage, including the 33–34 stage in the modified Eichorn-Lorenz (E-L) system (Coombe, 1995) labelled as pre-veraison (PV), and the 4 following phases of ripening from veraison labelled as Ripening-1 (R1), mid-ripening labelled as Ripening-2 (R2), harvest maturity (E-L 38 stage) labelled as Ripening-3 (R3), until over-ripe (E-L 39 stage) labelled as Ripening-4 (R4). The number of days after anthesis (DAA) on each sampling date for each cultivar was noted in Table 1.

TABLE 1. DAA and development stage in the Eichorn-Lorenz (E-L) system for each cultivar on the five sampling dates (PV, R1, R2, R3, R4).

Sampling Date	DAA and E-L Stage		
	Shiraz	Chardonnay	Flame Seedless
27/12/2019 (PV)	51 DAA, E-L 33	60 DAA, E-L 33	54 DAA, E-L 34
09/01/2020 (R1)	64 DAA, E-L 35	73 DAA, E-L 36	67 DAA, E-L 35
31/01/2020 (R2)	86 DAA, E-L 36	95 DAA, E-L 38	89 DAA, E-L 37
26/02/2020 (R3)	112 DAA, E-L 38	121 DAA, E-L 39	115 DAA, E-L 38
27/03/2020 (R4)	142 DAA, E-L 39	151 DAA, E-L 40	145 DAA, E-L 39

Grape berries were sampled every 4 hours from 5:00 to 21:00, resulting in 5 groups of samples from five time points on each sampling date. Fifteen samples were collected for each cultivar on one sampling date. All the cultivars were sampled at each time point within 30 min.

Figure 1 demonstrates the procedure of berry sampling and processing for each replicate at each sampling time point. Table 2 summarises the origin and number of berries collected for one replicate at each sampling time point. To provide a representative sample of the panels, the same number of berries were sampled from the eastern and western sides of the canopy at each sampling time point on every sampling date. Berry samples of each cultivar at each sampling time point were collected via the following sampling protocol. From the eastern side of the canopy, 3 to 9 berries were randomly collected using scissors from 3 to 9 random bunches in the same panel. One bunch provided one berry. Each vine in the same panel provided at least one berry from one side of the canopy. The same procedure was repeated from the western side of the canopy. Berries sampled from both sides of the canopy of the same panel were pooled as one replicate containing 6 to 18 berries. The procedure above was conducted in all cultivars 5 times on each sampling date.

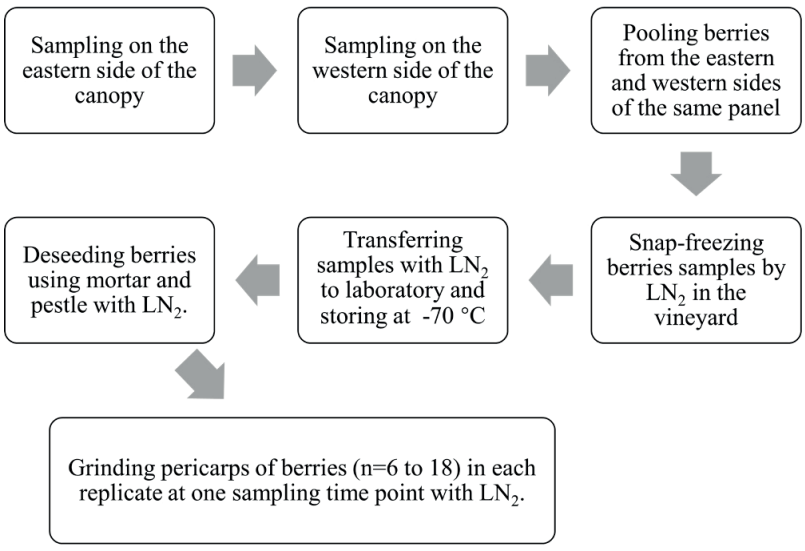


FIGURE 1. Grape berry sampling and processing for one replicate at each sampling time point.

TABLE 2. Origin and number of berries and replicates for Shiraz, Chardonnay and Flame Seedless at one sampling time point.

	Shiraz and Flame Seedless	Chardonnay
Berries from the eastern side of the canopy per replicate at one sampling time point	3 to 8 (PV and R1); 9 (R2 to R4)	3 to 8 (PV and R1); 9 (R2 to R4)
Berries from the western side of the canopy per replicate at one sampling time point	3 to 8 (PV and R1); 9 (R2 to R4)	3 to 8 (PV and R1); 9 (R2 to R4)
Total berries per replicate at one sampling time point	6 to 16 (PV and R1); 18 (R2 to R4)	6 to 16 (PV and R1); 18 (R2 to R4)
Replicates per sampling time point	3	3 (PV to R2) or 2 (R3 and R4)

Immediately after collection, the pooled berries from both sides of the vines were snap-frozen using liquid N_2 (LN_2) in the vineyard, then transferred under LN_2 to the laboratory and stored at -70 °C until processing and analysis. The frozen berries were deseeded and ground under LN_2. After seed removal by mortar and pestle, the frozen pericarps of the berries from each replicate were ground and homogenised using either TissueLyser II (QIAGEN) or IKA A11 analytical grinding mill (IKA) with LN_2. Homogenised pericarp samples were used for metabolite and inorganic element content analysis.

2. Pericarp water and inorganic element content determination

The frozen powdered pericarps (about 1 g) were weighed and dried at 60 °C for 10 days. The mass variation of the sample before and after drying was determined as the pericarp water mass. Dried pericarp samples were used to quantify the element contents, including Ca, K, Mg, Na and P, by inductively coupled plasma optical emission spectroscopy at the Environmental and Analytical Laboratories at Charles Sturt University. The pericarp K/Na ratio was obtained by dividing the K content by the Na content in the same pericarp sample.

3. Pericarp ATP content determination

ATP content was measured using a published method (Smyth and Black, 1984; Bajerski *et al.*, 2018; Köpnick *et al.*, 2018) with some modification. The mass of frozen powdery pericarp samples (100 to 120 mg) was measured and noted. Each frozen pericarp sample was extracted using 1 mL perchloric acid (0.83 M) on ice for 20 min. The extraction mixtures were buffered in 250 µL Bicine (1 M, pH 7.75 adjusted with 4M KOH) supplemented with PVP40 (50 mg/mL 1 M Bicine solution), followed by neutralisation to pH 7.2–7.8 using KOH (4 M) and litmus test paper (Whatman®, WHA2629990). The volumes of KOH (4 M) were noted. The neutralised extraction mixtures were centrifuged at 4 °C by 12,000 rcf for 10 min. The supernatants were collected as ATP extracts, and then stored at -20 °C until ATP determination. ATP standards prepared with Bicine (66 mM, pH 7.75 adjusted by 4 M KOH) were sterile-filtered and stored at -20 °C until ATP determination.

Kinase-Glo® Luminescent Kinase Assay (Promega, V6711) were used to analyse ATP concentration in the ATP standards and ATP extracts after two-fold dilution with autoclaved MilliQ water. ATP standard or diluted ATP extract (50 µL) was mixed with the reagent of Kinase-Glo® Luminescent Kinase Assay (50 µL) in a Nunc™ F96 MicroWell™ White Polystyrene Plate (Thermo Scientific™, 236105). The relative light units (RLU) of the luminescence reaction were measured using a Synergy™ HTX Multi-Mode Reader (BioTek) within 15 min after mixing samples and reagents. Luminescence (RLU) of ATP standards were used to generate the standard curves. Mass, water percentage, ATP extract volume and dilution factor of the pericarp sample were used to calculate pericarp ATP content and concentration.

4. Determination of pericarp ethanol, total sugar and L-malic acid content

The frozen pericarp samples were thawed, then their TSS was measured using a Pocket Refractometer (Atago, PAL-1) with a measurement range of 0–53 %. Juice was centrifuged at 15,000 rcf for 2 min, and then the supernatants (1 mL) were alkalised to pH 8–9 using KOH (10 M) and litmus test paper. The volume of KOH (10 M) that was added to alkalise the juice was noted in order to calculate the final sample volume. The pH-adjusted juice samples were used to determine ethanol, total sugar and L-malic acid concentrations in the pericarps. Ethanol was measured using a Thermo Scientific enzymatic assay kit (product code: CDK984300), 96-well microplates (Corning® Costar®, CLS3474) and a Synergy™ HTX Multi-Mode Reader (BioTek). Total sugar, quantified as the sum of sucrose, glucose and fructose, and L-malic acid were measured with Thermo Scientific enzymatic assay kits (product code: 984310 and 984317) using a Konelab (Arena X20, Thermo Fisher Scientific).

5. Data visualisation and statistical analysis

The data were processed and visualised using Excel and MATLAB R2022b (Version: 9.13.0.2105380). N-way analysis of variance (ANOVA) with two-way interactions and Type 3 sum-of-squares, multiple comparisons following ANOVA, correlation coefficient, linear regression and principal component analysis (PCA) were undertaken using MATLAB (R2022b). A two-way repeated measures ANOVA was performed for 3 explanatory factors with fixed effects, cultivar (CV), GDD, and time point of sampling (TPS), and a within-subjects factor with random effect, plant (PL). PCA was undertaken using mean centred and variance-scaled data block in MATLAB by singular value decomposition. In the two-way repeated measures ANOVA, the vine panel was considered as the observation unit sampled multiple times to compare the mean values of different cultivars throughout the ripening. The correlation coefficient, linear regression and PCA comprised the multiple variables collected on individual samples of the same cultivar, allowing us to descriptively analyse the patterns and relationships between variables in the same cultivar.

RESULTS

1. Cultivar variation in ripening parameters along with pericarp total sugar, L-malic acid, ATP and ethanol

Shiraz and Chardonnay pericarp fresh mass decreased during the later phases of ripening, mainly caused by dehydration instead of declining dry mass (Figure 2a) [Supplementary Information. Figure S2a, b]. The drop in water percentage (Figure 2b) and the rise in TSS [Supplementary Information. Figure S2c] were less extensive in the pericarp of Flame Seedless relative to the other two cultivars. The loss of pericarp water mass between 110 DAA (R3) and 150 DAA (R4) was significant in Shiraz only ($p < 0.0001$, Figure 2a). By contrast, an increase in pericarp total sugar content (Figure 2c) and dry mass [Supplementary Information. Figure S2b] from 110 DAA (R3) to 150 DAA (R4) was apparent in Flame Seedless ($p < 0.0001$). Pericarp water percentage varied significantly across TPS ($p = 0.0283$).

While total sugar per pericarp in Shiraz and Chardonnay did not change after 110 DAA, it increased continuously in Flame Seedless until the end of sampling (Figure 2c); however, the sugar concentrations of the three cultivars were similar as from around 100 DAA (Figure 2d). L-malic acid content dropped during berry ripening in all three cultivars with the greatest decline occurring before approximately 80 DAA (Figure 2e). The concentration and content of L-malic acid in the pericarp samples of Shiraz and Chardonnay approached their minimum at 110-120 DAA (Figure 2e, f), coinciding with the maximal total sugar content. Shiraz pericarps at 142 DAA (R4) contained less L-malic acid content ($p < 0.01$) and had a lower water mass ($p < 0.0001$) compared with 112 DAA (R3). The pericarp L-malic acid concentration in Flame Seedless at 54 DAA was only 20 % of those in the other two cultivars and was almost exhausted by 70 DAA (Figure 2f).

Cultivar differences were significant for pericarp ATP concentration and content ($p < 0.0001$). Pericarp ATP content increased progressively in Chardonnay and Flame Seedless from 55 DAA (PV). Shiraz contained the most stable ATP content throughout ripening (Figure 2g), while Chardonnay contained the highest pericarp ATP concentration and Shiraz contained the lowest (Figure 2h). Pericarp ATP concentrations were similar for all three cultivars before 70 DAA (R1). However, from 70 DAA onwards, ATP concentrations decreased in Shiraz but increased in Chardonnay and Flame Seedless. ATP concentrations varied significantly across TPS ($p = 0.0246$) as well as between biological replicates marked as PL ($p = 0.0423$).

The berry pericarp of all three cultivars contained low or undetectable ethanol until 70 DAA, with considerable cultivar variation in concentration and content on the last sampling date (Figure 2i, j). The cultivar significantly affected pericarp ethanol content ($p = 0.0149$) but did not impact ethanol concentration ($p = 0.3808$). Shiraz pericarp ethanol concentration fluctuated greatly in various ripening phases, increasing at 86 DAA (R2), followed by a drop at 112 DAA (R3), and eventually peaking at the highest value of the three cultivars at 142 DAA (R4) ($p < 0.0001$). Chardonnay pericarp ethanol concentration and content were lower than the other cultivars after 120 DAA ($p < 0.0001$). Flame Seedless pericarp contained higher concentration and content of ethanol than the other two cultivars before 70 DAA. Within the same sampling dates, there was extensive biological variation in pericarp ethanol for all cultivars, resulting from the significant variation across time points, as described in the diurnal patterns section below.

2. Cultivar variation in pericarp accumulation of inorganic cation elements during berry ripening

Three phloem-mobile elements, K, Mg and P, showed the fastest rate of accumulation in the ripening pericarp of Shiraz and Chardonnay between 70 and 90 DAA (R1-R2), followed by slow accumulation until completion on 110 DAA (R3) (Figure 3a, c, e). By contrast, the most rapid accumulation of these elements within the Flame Seedless pericarp occurred before 70 DAA (R1). K and P were the most abundant cations in all three cultivars. Shiraz pericarps contained higher concentrations of K and P than the other two cultivars from 140 DAA (R2) (Figure 3b, f). Pericarp content of Mg increased in Shiraz and Flame Seedless, but not in Chardonnay. Shiraz and Flame Seedless pericarp maintained relatively stable Mg concentration apart from a significant increase ($p < 0.0001$) in Shiraz at 142 DAA (R4) (Figure 3d). Chardonnay pericarp Mg concentration was the highest of the three cultivars ($p < 0.0001$) at 73-95 DAA (R1-R2); however, this was followed by a drop to the lowest amounts from 120 DAA onwards.

The pericarp content of the xylem-mobile elements, Ca and Na, slowly increased in Shiraz until 112 DAA and in Flame Seedless until 145 DAA (Figure 3g, i). However, Flame Seedless accumulated more Ca and had more variable Na contents. Although the contents of Ca and Na did not progressively accumulate in Chardonnay during ripening, increased Na content was detected between 70 to 95 DAA (R1-R2). Flame Seedless contained the highest Ca concentration at 55 DAA (PV), which dropped and remained stable after 65 DAA (R1) (Figure 3h). Calcium concentration in Shiraz and Chardonnay decreased from 70 DAA (R1), followed by cultivar-dependent fluctuations after 85 DAA (R2). Shiraz pericarp Ca concentration dropped to a minimum at 86-112 DAA (R2-R3), and then increased to the highest of the three cultivars ($p < 0.0001$) at 142 DAA (R4). Relative to the other cultivars, Chardonnay pericarp Ca concentration was lowest ($p < 0.0001$) from 121 DAA (R3) to 142 DAA (R4). Pericarp concentration of Na displayed a similar pattern to the Na content in the three cultivars (Figure 3j).

Chardonnay and Flame Seedless pericarps contained the highest and lowest ratios of K to Na respectively (Figure 3k). Flame Seedless maintained a stable pericarp K/Na ratio throughout berry ripening, while in Shiraz and Chardonnay, it decreased from 70 DAA onwards. After 95 DAA, the Shiraz pericarp K/Na ratio remained as low as that of Flame Seedless. However, in Chardonnay, the pericarp K/Na ratio recovered to the level apparent at 60 DAA.

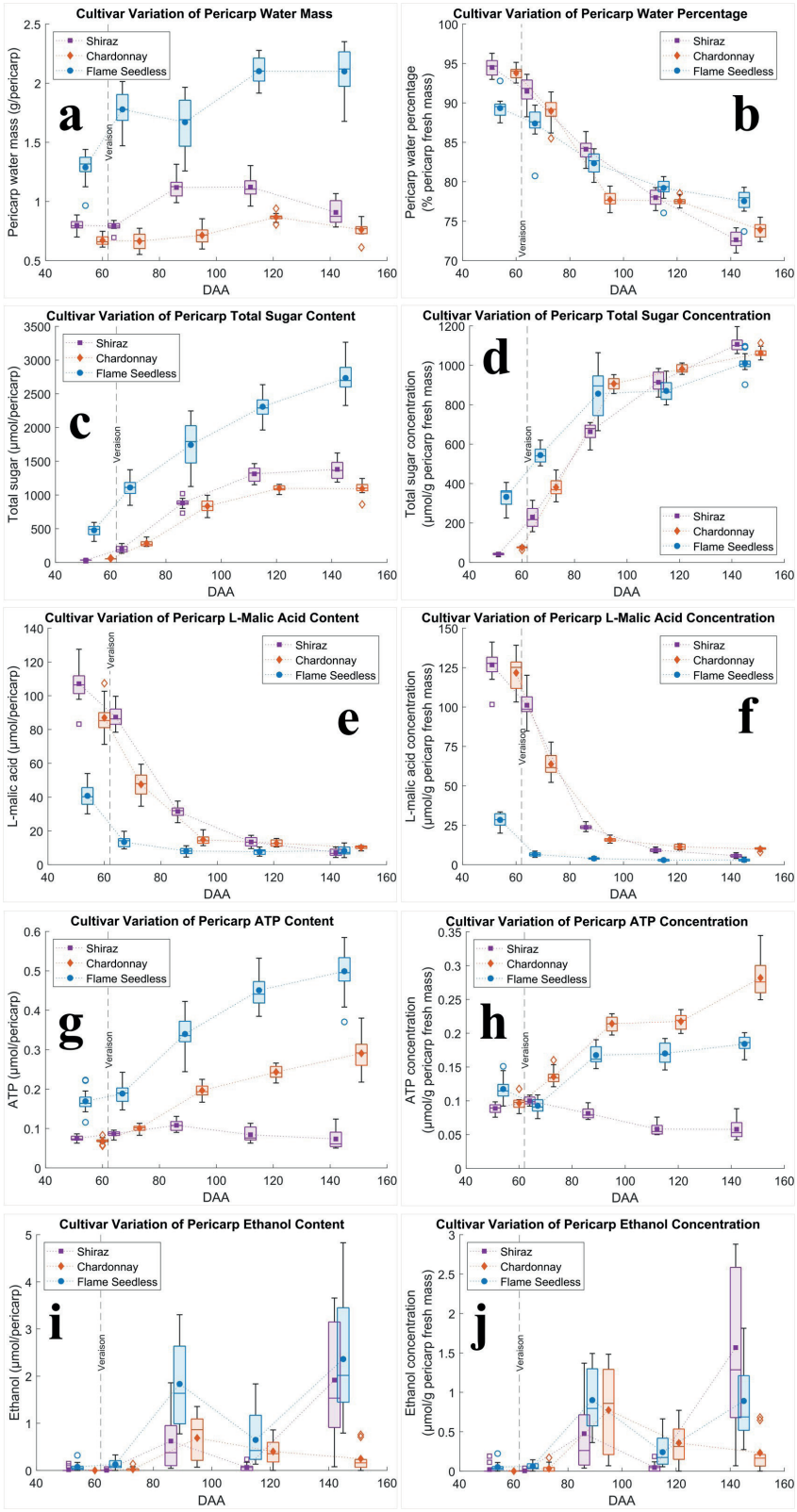


FIGURE 2. Cultivar variation in pericarp ripening parameters during grape berry ripening: water mass (a), water percentage (b), total sugar content (c) and concentration (d), L-malic acid content (e) and concentration (f), ATP content (g) and concentration (h), ethanol content (i) and concentration (j).

Data are shown as the group means (filled dots), and box charts of medians, lower and upper quartiles, minimal and maximal values other than any outliers, and outliers (unfilled dots) from the groups. Samples in each group were collected from 5 sampling time points on the same sampling date. For Shiraz (purple) and Flame Seedless (blue), each group contained 15 biological replicates. For Chardonnay (red), each group contained 15 biological replicates on the first 3 sampling dates, and 10 replicates on the last 2 sampling dates. Each replicate contained the homogenised pericarps of 6 to 18 berries. Vertical dash lines indicate the initiation of veraison.

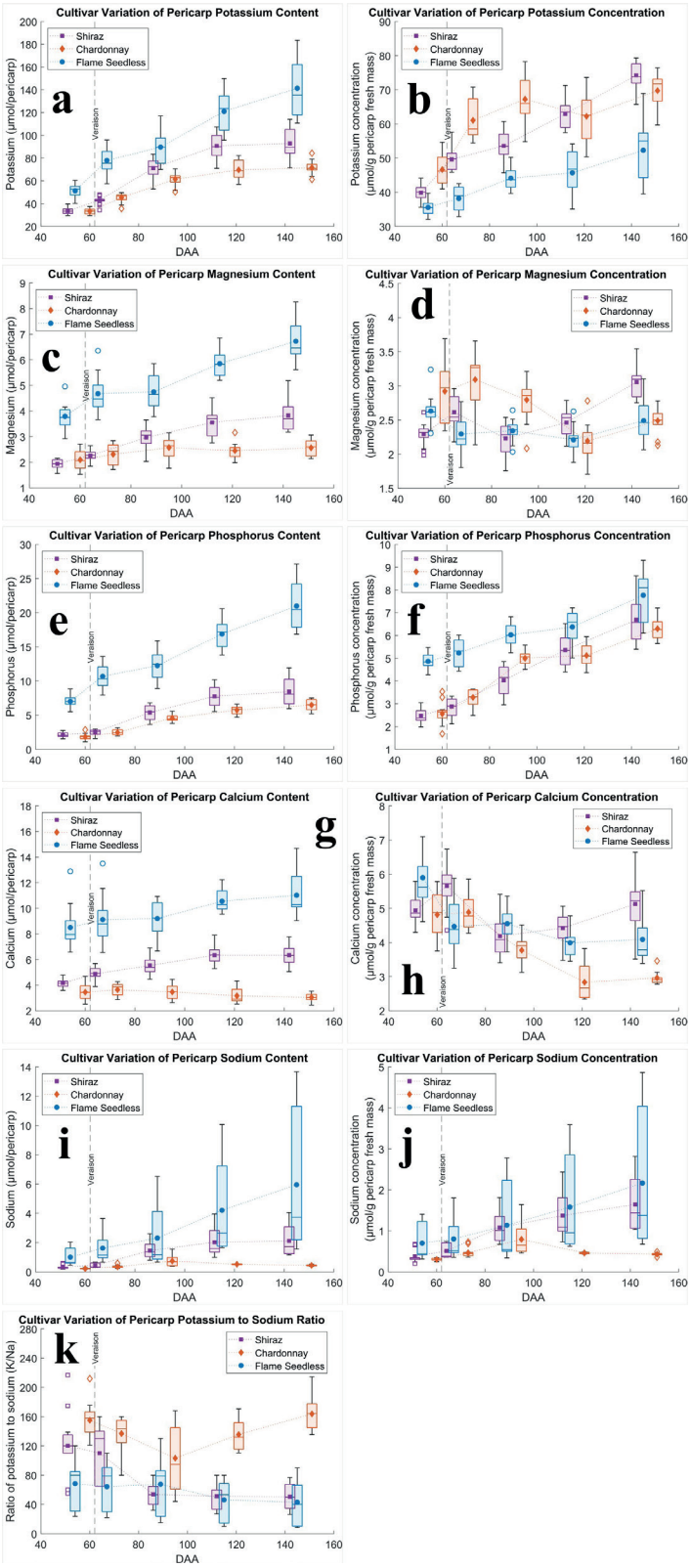


FIGURE 3. Cultivar variation in the cation elements: K content (a) and concentration (b), Mg content (c) and concentration (d), P content (e) and concentration (f), Ca content (g) and concentration (h), Na content (i) and concentration (j), and the K/Na ratio (k) in pericarps during grape berry ripening.

Data are shown as the group means (filled dots), and box charts of medians, lower and upper quartiles, minimal and maximal values other than any outliers, and outliers (unfilled dots) from the groups. Samples in each group were collected from 5 sampling time points on the same sampling date. For Shiraz (purple) and Flame Seedless (blue), each group contained 15 biological replicates. For Chardonnay (red), each group contained 15 biological replicates on the first 3 sampling dates, and 10 replicates on the last 2 sampling dates. Each replicate contained the homogenised pericarps of 6 to 18 berries. Vertical dash lines indicate the initiation of veraison.

3. Diurnal profile of pericarp parameters in three cultivars at five ripening phases

The diurnal patterns of ATP and ethanol concentrations (Figure 4), as well as the pericarp water percentage and the concentrations of total sugar, L-malic acid and K [Supplementary Information. Figure S3] depended on cultivar and berry maturity on a particular sampling date, as indicated by the interaction between TPS and GDD [Supplementary Information. Table S1]. Pericarp ATP concentrations were relatively stable across time points on individual sampling dates, although the samples at 5:00 at R4 tended to contain higher ATP concentrations in all three cultivars (Figures 4a, c and e). While pericarp ethanol concentrations in all the cultivars increased between 13:00 to 21:00 at R2, they decreased during this time at R3 (Figure 4b, d, f). Similar diurnal trends in ethanol concentration were evident in each cultivar at R2 and R3. At R2 and R3, ethanol concentrations did not alter significantly in any of the cultivars before 13:00. In Chardonnay at R2, pericarp ethanol concentration at 17:00 was significantly higher than at 9:00 ($p = 0.0023$). In Chardonnay at R4, the pattern of ethanol concentration was similar to that of R2, peaking in the afternoon. Conversely, in Shiraz and Flame Seedless at R4, the highest ethanol concentrations were detected at 9:00.

4. Principal component analysis of pericarp parameters associated with cultivar and maturity

Given the dominating attributes of sugar and L-malic acid relative to the other parameters assessed, a PCA was carried on the pericarp concentrations of ATP, ethanol, inorganic elements and the ratio of pericarp K/Na (Figure 5). The scores of the PCA (Figure 5a) indicate that principal component (PC) 1 (31 %) separates the sampling dates, while PC2 (24 %) separates Chardonnay and half of the Flame Seedless samples in opposite directions largely due to the K/Na ratio and Na concentration (Figure 5b). The patterns of ATP and K concentrations may be correlated.

5. Relationships between pericarp parameters varied with cultivar and ripening phase

As indicated by the larger and coloured circles in Figure 6, the correlations between the inorganic elements and the other parameters are stronger in Shiraz (Figure 6a) than in the other two cultivars (Figure 6b, c), except in the case of K and P content. By contrast, strong correlations between ATP and the other parameters were observed in Chardonnay. In the pericarps of all three cultivars, a lower K/Na ratio was positively correlated with total sugar concentration, Mg content and Ca content, but negatively correlated with water percentage and L-malic acid concentration. The above correlations with the K/Na ratio were most significant in Shiraz, as indicated by the largest circles representing the smallest p values of the three cultivars. Shiraz pericarp K/Na ratio was also significantly correlated with various parameters, including TSS and ATP concentration, as well as P concentration and content, which were not evident in the other two cultivars. In cultivars with seeds, berry seed number was not strongly correlated with the other measured parameters in Shiraz, but was positively or negatively correlated with other parameters in Chardonnay. Ethanol concentration and content, as well as the time point of sampling, did not appear to be well-correlated with any other parameters in all cultivars.

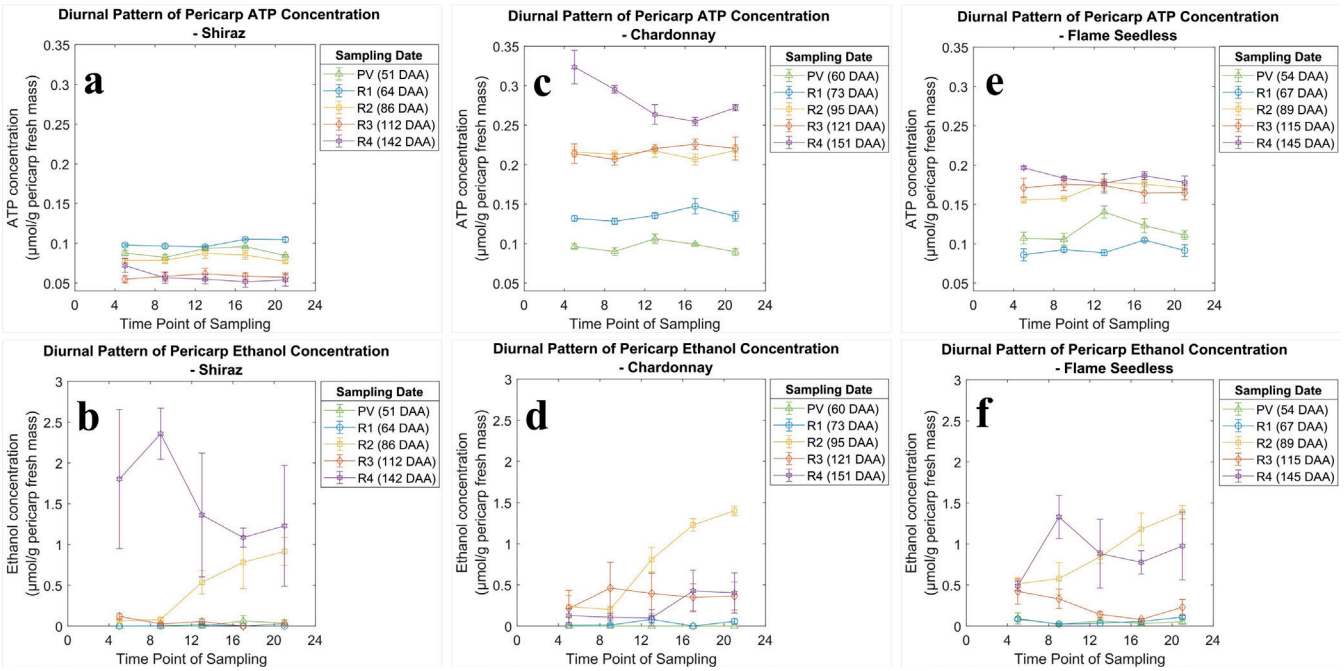
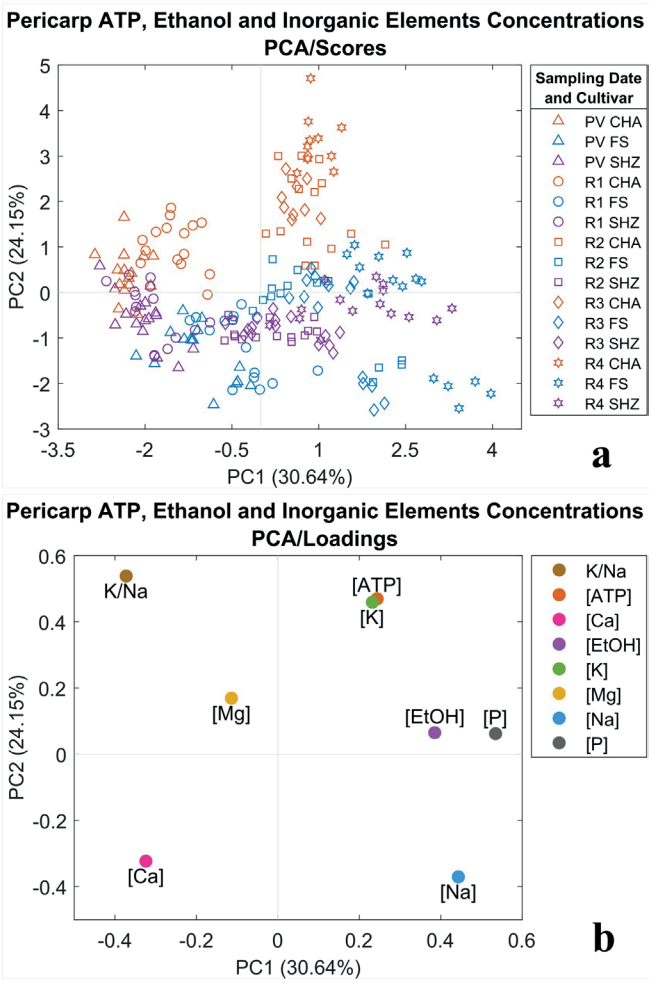
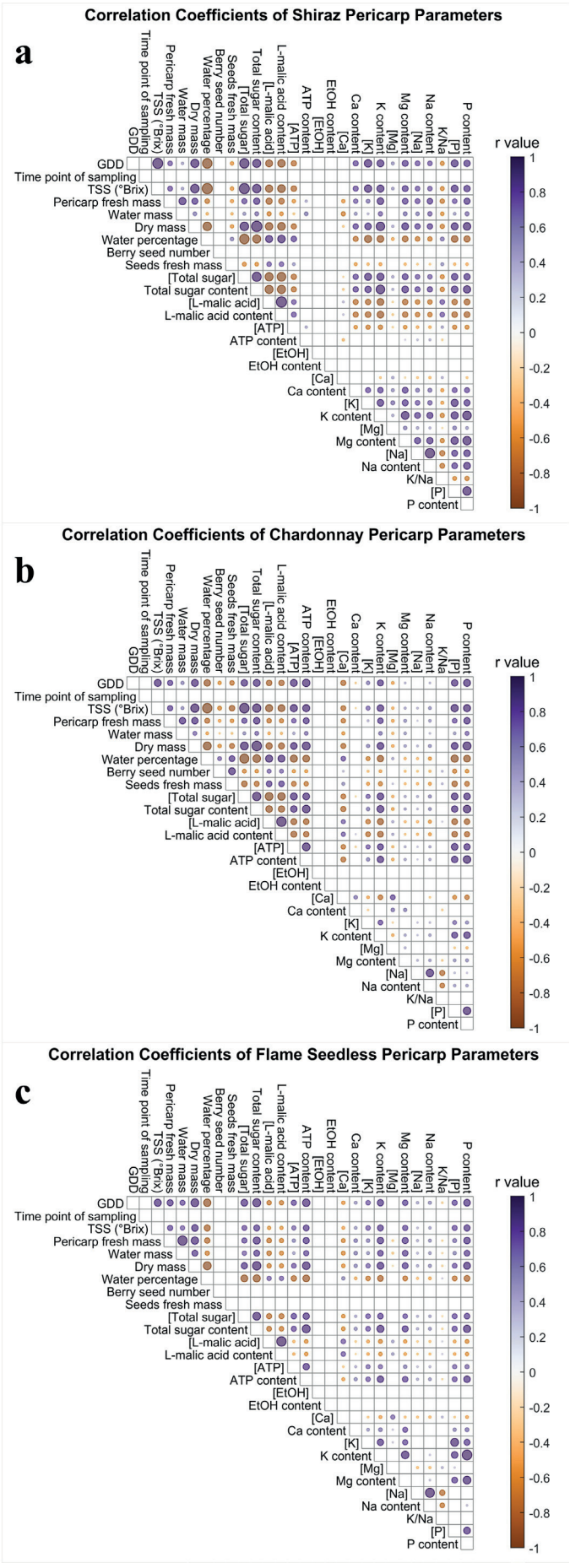


FIGURE 4. Diurnal patterns of pericarp concentrations of ATP and ethanol in Shiraz (a, b), Chardonnay (c, d) and Flame Seedless (e, f).

On R2 (yellow), Chardonnay pericarp ethanol concentration at 17:00 was significantly higher than at 9:00 ($p = 0.0023$). In Shiraz and Flame Seedless, each data point represents the mean value of 3 replicates. In Chardonnay, each data point represents the mean value of 3 replicates in PV, R1 and R2, and the mean value of 2 replicates in R3 and R4. Each replicate contains the homogenised pericarps of 6 to 16 berries in PV and R1, and 18 berries in R2 to R4. Error bars indicate the standard error of the mean (n=3 or 2).



▲ **FIGURE 5.** Characterisation of solutes in Shiraz, Chardonnay and Flame Seedless pericarps by PCA of the concentrations of ATP, ethanol and cation elements, as well as the K/Na ratio of the pericarp. Chardonnay pericarps were distinguished as having the highest K/Na ratio, ATP and K concentrations throughout ripening, as well as the highest Mg concentration in the early ripening stages. Shiraz and Flame Seedless pericarps contained higher ethanol and Na concentrations in later ripening stages.



▶ **FIGURE 6.** Correlation coefficients of all assessed pericarp parameters in Shiraz (a), Chardonnay (b) and Flame Seedless (c). The size of circles is the absolute value of $\log_{10}(p)$, thus the more significant the correlation, the larger the circle. The insignificant data ($p > 0.05$) are not shown. Ethanol concentrations and contents below the detection limit were removed before the cross correlation analysis.

DISCUSSION

1. Berry pericarp solute accumulation varied with cultivar and ripening phase, as reflected by pericarp water content and elements with xylem or phloem mobility

From the onset of ripening, grape berries become sinks for water and various solutes, including sugar and minerals, by way of translocation through vascular tissues (Rogiers *et al.*, 2006a; Rogiers *et al.*, 2006b). Solute accumulation ceased in Shiraz and Chardonnay in the later stages of ripening (Figure 2, 3), which is supported by previous publications (Rogiers *et al.*, 2006a; Rogiers *et al.*, 2006b). Prior to the cessation in phloem unloading, berry water removal via transpiration across the skin and backflow through the xylem was required to enable soluble solids accumulation and a skin colour change (Zhang and Keller, 2017). Berry shrivel during late ripening in Shiraz may be associated with the cessation in phloem unloading, transpiration and possibly backflow to the vine (Tyerman *et al.*, 2004; Greer and Rogiers, 2009). Without phloem inflows, the occurrence of transpiration and backflow may induce berry dehydration and shrinkage.

Most pericarp parameters assessed in this study responded to GDD [Supplementary Information. Table S1], indicating that solute accumulation and energy status were mainly driven by maturity. However, cultivar-associated dynamics of water and solute accumulation during berry ripening indicate that vascular inflows were unique for each cultivar. The pericarp of Shiraz and Chardonnay experienced greater percentages of water than those of Flame Seedless before 90 DAA (Figure 2b). However, rapid declines in water content (Figure 2a) for Shiraz and Chardonnay resulted in a less hydrated pericarp beyond 110 DAA. It is likely that cessation in berry water importation, as inferred from changes in berry water mass, occurred at approximately 90 DAA in Shiraz, but not until 30 days later in the other two cultivars. Unlike Shiraz and Chardonnay, pericarp dry mass [Supplementary Information. Figure S2b] and sugar content (Figure 2c) increased significantly in Flame Seedless after 110 DAA, signifying continued phloem unloading. This was supported by the progressive accumulation of K, Mg and P until 142 DAA in Flame Seedless, but only until 110 DAA for the other cultivars (Figure 3a, c, e). The absence of berry shrivel in Flame Seedless may be due to continued phloem unloading, while the combination of transpiration and xylem backflow after the cessation in phloem unloading may contribute to the more apparent berry shrivel in Shiraz.

2. Pericarp ATP and ethanol contents may be linked to the changes in berry energy status

Grape berry ripening requires energy in the form of ATP, inorganic pyrophosphate (PP_i) and electrochemical gradients of solutes and ions (Terrier *et al.*, 1998; Gajdanowicz *et al.*, 2011; Igamberdiev and Kleczkowski, 2021). ATP is most efficiently generated under aerobic conditions by mitochondria. It has been reported that in postharvest pear and apples, ATP concentration decreased and was associated with fatty acid and lipid metabolism, loss in membrane integrity and fruit physiological disorders during storage (Saquet *et al.*, 2000; Saquet *et al.*, 2003). In addition, treating postharvest longan fruit with ATP inhibited the decrease of sugar and vitamin C, and delayed the progressive loss of cell membrane integrity (Chen *et al.*, 2015). These studies suggest that ATP may have a pivotal role in grape berry maturation and cell membrane integrity. While ATP content continued to increase in Flame Seedless and Chardonnay until 140 DAA, Shiraz pericarp ATP content ceased to increase beyond 86 DAA and subsequently declined (Figure 2g). By the next sampling date, sugar (Figure 2c) and the phloem mobile elements (Figure 3a, c, e) also ceased to accumulate in Shiraz which is prone to pericarp dehydration, low O_2 levels and mesocarp cell death (Tilbrook and Tyerman, 2008; Xiao *et al.*, 2018b). This reduction in ATP suggests there was an energy loss in the Shiraz berry, which may be associated with berry cell vitality loss promoted by hypoxia (Xiao *et al.*, 2018b): without sufficient O_2, the ability of cells to continue aerobic respiration is compromised and may trigger anaerobic processes, such as fermentation, with less efficient energy production and the formation of ethanol.

The changes in pericarp ethanol concentration and content during ripening indicate a change in fermentation activity and potential energy status of the berries. Fermentation has been found to accelerate in ripening grape berries deficient in O_2 (Famiani *et al.*, 2014; Xiao *et al.*, 2018b). The ethanol concentrations and content of all three cultivars increased from 86-95 DAA (R2) onwards ($p < 0.05$) (Figure 2i, j), with TSS of 15 - 20 °Brix [Supplementary Information, Figure S2c], coinciding with a decreased rate of phloem-mobile solute accumulation after 85 DAA (Figure 3a, c, e). The augmentation in fermentation suggests its increased contribution to energising berries during this ripening phase. Slow solute accumulation, which coincided with promoted fermentation with low ATP production efficiency, suggests there was an imbalance of limited ATP production and increased energy requirements for overcoming solute gradients. Relative to the other cultivars, Shiraz had the highest ethanol concentration at 142 DAA (R4). Conversely, Tilbrook and Tyerman (2008) found table grape berries to maintain high cell vitality until harvest maturity, which could explain the high pericarp ATP content in Flame Seedless throughout berry ripening. Additionally, solute accumulation continued until 145 DAA in Flame Seedless (Figure 2, Figure 3). Unexpectedly, the Flame Seedless pericarp also contained increased ethanol in the later ripening stages (Figures 2i and j), which may be associated with the larger berries of Flame Seedless. A high level of accumulated ethanol could be attributed to not only a high production rate but also a low evaporation rate. The distance from berry centre to the skin increases with berry size, meaning that ethanol evaporation in Flame Seedless was slower with larger berry volumes. Large berry volumes could inhibit O_2 penetration to the deeper cell layers, similar to the hypoxia present within the central mesocarp tissue of Shiraz (Xiao *et al.*, 2018b). Ethanol may be formed within these deeper layers and undergo slow evaporation, while tissues closer to the periphery may experience higher O_2 levels and are therefore able to

maintain phloem unloading from the peripheral vascular network and thus solute accumulation. Thus, vital and active vascular tissue in Flame Seedless may be the contributor in maintaining berry energy and accumulating solutes in late ripening phases. An assessment of the O_2 profile through Flame Seedless and other large berried cultivars would shed light on this issue. Environmental conditions on the day of sampling and bunch exposure may impact berry temperature and thus respiration rates and ethanol volatility; further assessments would be required to corroborate this.

3. Diurnal fluctuation of pericarp parameters may impact berry water and energy status

The diurnal rise and fall of solutes and metabolite concentrations may reflect the balance of production and consumption at any time point in the 24-hour cycle. Furthermore, longer-term changes across the season could reflect the integration of the daily balance and may signify overall changes in energy status and maturity progression. Berries sampled at various time points on the same day differed significantly in hydration status and ATP concentration [Supplementary Information. Table S1]. Additionally, two-way interactions between GDD and TPS were significant in the variation in these two parameters, as well as the pericarp concentration of total sugar, L-malic acid, K and ethanol. A significant two-way interaction indicates that the diurnal patterns were related to berry maturity. Thus the effect of environmental factors on berry hydration and energisation could vary depending on ripening phases. Since climate warming is accelerating berry ripening and shortening the growing season, grape berries are showing a tendency to ripen in the period with longer daytime and higher temperatures. The impacts of longer daytime and heat on riper berries are still unclear. It is possible that diurnal variation in berry hydration and energisation is cumulative and impacts berry hydration and energisation in the long term.

The variation in pericarp ethanol concentration across time points indicates that fermentation activity was uneven during the day (Figure 4b, d, f), possibly because of temperature fluctuations. Apart from fermentation activity, there are many factors that may influence the concentration of pericarp ethanol, including berry O_2 concentration, wind and air. These various internal and external parameters, sensitive to environmental factors and berry metabolism, require further assessment to better understand their roles and contributions.

Pericarp hydration, and thus the concentration of solutes within the cells, are likely responsive to daily changes in light, temperature, vapour pressure deficit and thus berry transpiration. During the transition from dark to light, a net uptake of K^+, correlated with of H^+ and Ca^{2+} fluxes, was evident in grape mesocarp tissue and potentially associated with the membrane voltage generated by contributions of ATP (Shabala and Wilson, 2001). In addition, sugar and K^+ are imported into the pericarp via translocation, a function of vascular activity, vascular concentration and partitioning patterns. It has been hypothesised that vascular flow supplies O_2 to support berry respiration (Xiao *et al.*, 2018b), thus possibly improving the ATP generation rate. However, ATP consumption may increase because of active phloem unloading and solute transport. Since phloem unloading switches to the apoplasmic pathway at the onset of ripening (Zhang *et al.*, 2006), solute transport into and accumulation within berry cells involves active transport across cell membranes that are either energised by ATP or by the H^+ gradients resulting from H^+ pumps that consume ATP or PP_i. Balanced ATP generation and consumption may explain the stable ATP concentration in the pericarp at various time points on the same sampling date (Figure 4a, c, e).

4. Element accumulation patterns within grape berries may be associated with links between ionic homeostasis and energisation

Plant energetics relies on ions which assist cellular energisation by maintaining electrochemical gradients across the membranes or interacting with ATP molecules. There is a high demand for energy to enable sugar accumulation in the ripening grape berries under hypoxia (Savoi *et al.*, 2021). The accumulation patterns of K, P, Mg and Ca indicate that the importation of these elements could contribute to berry energisation in the late ripening phase.

Potassium was the most abundant element in the ripening grape berries (Figure 3a, b); this may be associated with the role of K in energy, supported by that K^+ gradients across the plasma membrane could assist in energising the phloem loading with ATP limitation (Gajdanowicz *et al.*, 2011). Phosphorus accumulation in the berries may have contributed to the highly active solute transport for berry maturation (Figure 3e), since P is present in energy molecules in plants, such as ATP, adenosine diphosphate (ADP), and PP_i (Prathap *et al.*, 2022). Increased P supply has been found to improve the plasma membrane energisation and the uptake of K^+, Ca^{2+} and Mg^{2+} in green beans (Salinas *et al.*, 2013). The relatively stable concentration of Ca and Mg (Figure 3d, h) may be associated with the stable ATP concentration during berry ripening. In cells during a stress response, increased extracellular ATP and ADP raise the Ca^{2+} concentration (Clark and Roux, 2018). Reactive oxygen species (ROS) have been shown to induce Ca^{2+} influx and trigger programmed cell death (Demidchik, 2018). Cell vitality loss in Shiraz berries with progressive hypoxia (Xiao *et al.*, 2018b) may be a result of Ca^+ transport linked to ROS (Demidchik and Shabala, 2018) and extracellular ATP (Sun *et al.*, 2012; Clark and Roux, 2018; Hou *et al.*, 2020). Shiraz pericarp Mg concentration increased after 112 DAA (R3) (Figure 3d), which may have assisted berry energisation as the cofactor role of Mg to ATP and PP_i (Igamberdiev and Kleczkowski, 2001, 2011). Magnesium is physiologically bound with ATP and ADP (Igamberdiev and Kleczkowski, 2001). Therefore, under oxygen (O_2) deficiency with reduced ATP concentration, free Mg^{2+} concentration may increase and promote the usage of PP_i as an alternative energy source in $MgPP_i$ and Mg_2PP_i, thus increasing energy efficiency by saving ATP and activating Mg^{2+}-dependent enzymes (Igamberdiev and Kleczkowski, 2011).

Changes in the pericarp K/Na ratio during ripening suggest that K^+ and Na^+ transport into and accumulation within berries was regulated differently and depended on cultivar

and berry maturity level (Figure 3k). Plants can benefit from an adequate concentration of Na^+, because, transported through some K^+ transporters and channels, it regulates osmotic pressure (Maathuis, 2014). However, excessive Na^+ can induce salinity stress and cell death (Azhar *et al.*, 2017). Sodium ions are transported to the shoot through xylem (Jeschke *et al.*, 1992), but are also capable of transport through the phloem (Munns, 2002), explaining the continued increase in Na content in Shiraz and Flame Seedless (Figure 3i). Significant xylem flow into the berries was found to cease in Chardonnay after veraison (Tilbrook and Tyerman, 2009). The cessation of xylem inflow could limit Na^+ importation into berries, which might have contributed to Chardonnay's high pericarp K/Na ratio relative to the other two cultivars. A stable and low pericarp K/Na ratio was maintained in Flame Seedless throughout berry ripening, possibly associated with the continued K^+ and Na^+ importation through functioning phloem and xylem until the last sampling date evident in this study. The Shiraz pericarp K/Na ratio decreased after veraison, indicating that the transport of K^+ and Na^+ into and within berries was altered by factors associated with the progression of berry maturation. Developmental patterns of the pericarp K/Na ratio were possibly associated with dynamic solute accumulation during berry ripening.

The optimal pericarp K/Na ratio and ionic homeostasis can be achieved by the fine regulation in the intercellular and intracellular transport of K^+ and Na^+. Both K^+ and Na^+ are transported by high-affinity K^+ carriers and non-selective cation carriers, but Na^+ is unable to support the cellular metabolic functions requiring K^+ as an enzyme cofactor (Maathuis and Amtmann, 1999). Excessive Na^+ could lead to the loss of cell vitality (Azhar *et al.*, 2017), partly because of the insufficiency of K^+ with important cofactor role for many enzymes including those essential for ATP production, such as pyruvate kinase (Oria-Hernández *et al.*, 2005) and succinyl-CoA thiokinase (Cui and Tcherkez, 2021). A grape berry vacuolar cation/H^+ antiporter contributes to K^+ and Na^+ accumulation (Hanana *et al.*, 2007). Vacuolar pH values impacts the K^+ selectivity of the Arabidopsis cation/H^+ antiporter AtNHX1, reducing the activity of K^+/H^+ relative to Na^+/H^+ by increased pH values (Bassil and Blumwald, 2014). It is possible that the K^+ selectivity of tonoplast cation/H^+ antiporters in grape berries are altered by vacuolar alkalinisation during berry ripening (Terrier *et al.*, 2001). Increased activity of vacuolar H^+ pumps have been detected in ripening berries of Ugni Blanc (Terrier *et al.*, 1997). Furthermore, the abundance of various vacuole transport proteins was found to increase or decrease during berry ripening (Kuang *et al.*, 2019). The dynamic nature of these proteins shows that solute transport across the tonoplast is highly complex. The proposed high sensitivity of Shiraz to K^+ and Na^+ homeostasis suggests its susceptibility to ion disorder under stress and ATP shortage.

The correlation between the Shiraz pericarp K/Na ratio and the pericarp parameters was the most significant, as indicated by the lower p values represented by larger circles in the correlation coefficient plots (Figure 6). These correlations suggest that K^+ and Na^+ homeostasis may be more sensitive to parameter alteration in Shiraz. Significant correlations between the K/Na ratio and ATP concentration and content in Shiraz pericarps indicate that the berry's energy status may affect the regulation of K^+ and Na^+ transport across energised cell membranes. Linked with solute transport and energy regulation, the reduced pericarp K/Na ratio in the later ripening phases of Shiraz might be associated with the loss of mesocarp cell vitality in maturing berries (Tilbrook and Tyerman, 2008). However, little is known about the maintenance of the K/Na ratio in grape berries, as well as the homeostasis of K^+ and Na^+ in berry cells. To our knowledge, the dynamics between K^+ and Na^+ transport has not yet been assessed during berry development, but it is worth investigating as it may contribute to K^+ transport regulation, as well as to metabolism alteration in grape berries.

Further investigations into intracellular and intercellular ion transport and homeostasis in grape cultivars with various energy statuses and metabolic features could provide insight into cellular regulation in metabolism and vitality in grape berries. Future studies would be required to evaluate and confirm the potential associations between ionic homeostasis and cell energisation in ripening grape berries as discussed in the present study.

5. Energy limitation and ionic disorder may contribute to Shiraz berry weight loss in the later ripening phase

Sufficient energy and essential ions are important for maintaining cell vitality. Berry dehydration and shrivel - associated with berry cell death - in the late-ripening phase in the Shiraz mesocarp has been found to be accelerated by elevated temperature and water deficiency (Bonada *et al.*, 2013a; Bonada *et al.*, 2013b; Xiao *et al.*, 2018a), as well as by berry hypoxia exacerbated by lenticel blocking (Xiao *et al.*, 2018b). K^+ is the most abundant cation in cells and berries (Rogiers *et al.*, 2017), which ceases to accumulate within Shiraz berries in the late-ripening phase (Rogiers *et al.*, 2006a; Rogiers *et al.*, 2006b). The present study found potential associations between Shiraz pericarp ATP, K and the K/Na ratio (Figure 5, Figure 6). A study has demonstrated that K^+ can stimulate the dephosphorylation of plasma membrane H^+-ATPase and regulate plasma membrane voltages in Arabidopsis (Buch-Pedersen *et al.*, 2006). Plants with improved salt tolerance have been found to have a higher K^+/Na^+ ratio in shoots than in roots (Wang *et al.*, 2021). Since K^+ is the enzyme cofactor (Maathuis and Amtmann, 1999), the concentration of K^+ and the ratio of K^+ to Na^+ may impact cellular metabolism and ultimately regulate cell vitality. These studies provide further support for the potential links between energy and ionic homeostasis in ripening Shiraz berries.

Given that berry hypoxia and the cessation of solute accumulation are associated with Shiraz berry shrivel (Rogiers *et al.*, 2006a; Xiao *et al.*, 2018b), ATP limitation and ionic disorder revealed by the present study may have contributed to these physiological changes during late ripening (Figure 7). Chardonnay and Flame Seedless, two

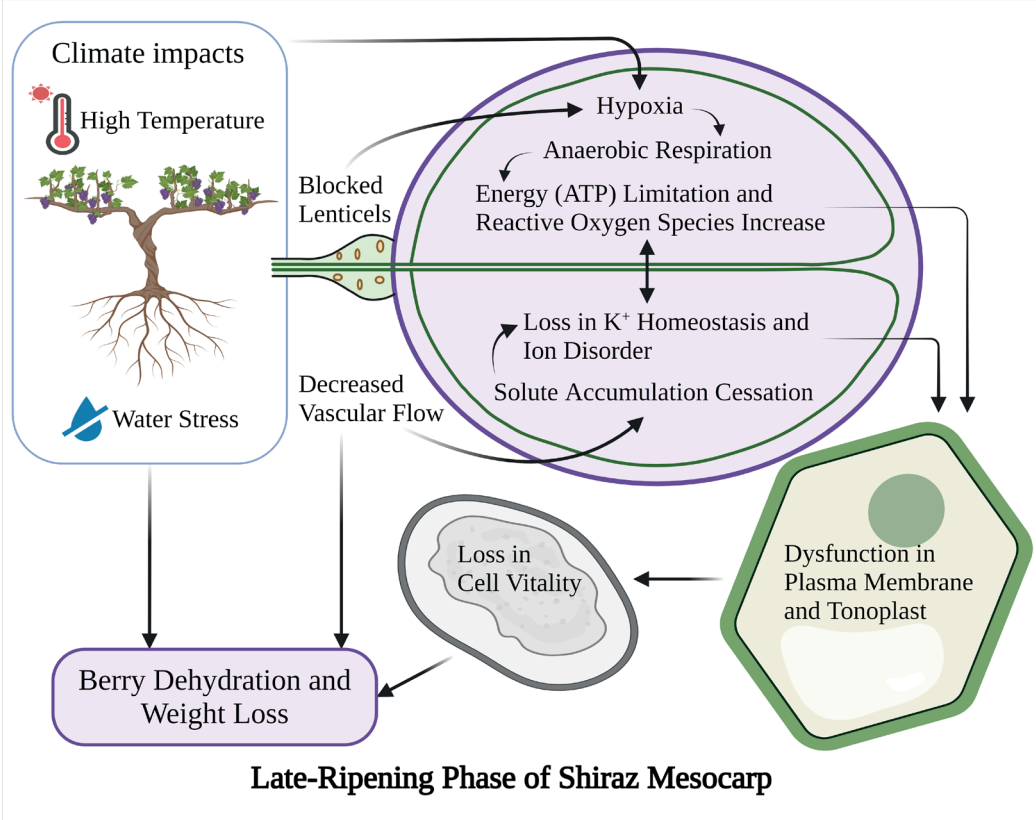


FIGURE 7. The ATP limitation and ionic disorder indicated by the present study, along with other physiological processes, may contribute to Shiraz berry weight loss during the later berry ripening phase. Heating, drying, lenticel blocking and slowed vascular inflow were found to enhance berry dehydration and cell death in Shiraz in the later stage of ripening (Bonada *et al.*, 2013a; Bonada *et al.*, 2013b; Rogiers *et al.*, 2006a; Xiao *et al.*, 2018a; Xiao *et al.*, 2018b). The figure was created with BioRender.com.

cultivars that did not undergo significant berry weight loss in the later ripening phase, did not show reduced ATP levels or K/Na ratios. By contrast, the significant berry weight loss characteristic of Shiraz may be due to the decline in ATP availability and ionic homeostasis. Further studies on the cellular and molecular events during energisation loss, and the cellular responses to energy limitation are required to assess and confirm these proposed mechanisms related to K function and cellular energisation in ripening grape berries.

CONCLUSION

With the aim of determining the potential contributors to cultivar-dependent berry shrivel and mesocarp cell death in grape berries, variations in pericarp parameters (fresh mass, dry mass, water mass and percentage, TSS, sugar, L-malic acid, ATP, ethanol, five inorganic elements indicating vascular flows, and K/Na ratio linked to ionic homeostasis and metabolism) were analysed across three cultivars, five ripening phases and five time points during the day-night cycle. These parameters changed significantly with maturity in the three cultivars displaying different levels of berry shrivelling and cell death in the late ripening stage, which supported the hypothesised link between berry hydration, solute accumulation and energisation. Anaerobic respiration along with a sufficient supply of inorganic elements may have met the energy demands for solute accumulation within the pericarp for maturation. The developmental pattern of pericarp K/Na ratio was cultivar dependent, suggesting that the intracellular transport and compartmentation of K^+ and Na^+ may be associated with berry hydration, energisation and cell vitality. Shiraz was distinguished by significant water loss from the pericarp after solute accumulation ceased, progressive reduction of ATP concentration and content during berry ripening; furthermore, closer correlations between the K/Na ratio and other pericarp parameters indicate that energy loss and K/Na regulation may have contributed to the aforementioned significant berry dehydration and cell death. The pericarp of Chardonnay berries continued to accumulate ATP after solute accumulation had ceased. This cultivar also had the highest K/Na ratio with fewer impactors than the other two cultivars, possibly associated with cell vitality maintenance and the lowest xylem inflow during berry ripening. The pericarp of Flame Seedless berries did not lose water or finish solute accumulation, indicating that vascular transport and solute accumulation contributed to berry hydration. Time of day affected pericarp water percentage and ATP concentration, which may reflect the diurnal variation of vascular transport and energy regulation in berries. The variations in pericarp energy status and solute accumulation regulation may affect cell vitality during grape berry ripening, potentially contributing to berry water loss.

AUTHOR CONTRIBUTION STATEMENT

Conceptualisation: YL, SYR and SDT; methodology: SYR, SDT and YL; analysis and data visualisation: YL and LMS; writing of original draft: YL; writing, reviewing and editing: SYR, SDT, LMS and YL; supervision: SYR, SDT and LMS.

ACKNOWLEDGEMENTS

The authors thank Helen Pan (Charles Sturt University) and Wendy Sullivan (University of Adelaide) for laboratory arrangements and technical assistance. This research was supported by the Australian Research Council Training Centre for Innovative Wine Production (www.ARCwinecentre.org.au; project number IC170100008), funded by the Australian Government with additional support from Wine Australia, Charles Sturt University, and industry partners, as well as the Gulbali Research Institute. The University of Adelaide is a member of the Wine Innovation Cluster.

REFERENCES

Azhar, N., Su, N., Shabala, L., & Shabala, S. (2017). Exogenously applied 24-epibrassinolide (EBL) ameliorates detrimental effects of salinity by reducing K^+ efflux via depolarization-activated K^+ channels. *Plant & Cell Physiology*, *58*(4), 802-810. https://doi.org/10.1093/pcp/pcx026

Bajerski, F., Stock, J., Hanf, B., Darienko, T., Heine-Dobbernack, E., Lorenz, M., Naujox, L., Keller, E. R. J., Schumacher, H. M., Friedl, T., Eberth, S., Mock, H. P., Kniemeyer, O., & Overmann, J. (2018). ATP content and cell viability as indicators for cryostress across the diversity of life. *Frontiers in Physiology*, *9*, Article 921. https://doi.org/10.3389/fphys.2018.00921

Bassil, E., & Blumwald, E. (2014). The ins and outs of intracellular ion homeostasis: NHX-type cation/H^+ transporters. *Current Opinion in Plant Biology*, *22*, 1-6. https://doi.org/10.1016/j.pbi.2014.08.002

Bonada, M., Sadras, V., Moran, M., & Fuentes, S. (2013a). Elevated temperature and water stress accelerate mesocarp cell death and shrivelling, and decouple sensory traits in Shiraz berries. *Irrigation Science*, *31*(6), 1317-1331. https://doi.org/10.1007/s00271-013-0407-z

Bonada, M., Sadras, V. O., & Fuentes, S. (2013b). Effect of elevated temperature on the onset and rate of mesocarp cell death in berries of Shiraz and Chardonnay and its relationship with berry shrivel. *Australian Journal of Grape and Wine Research*, *19*(1), 87-94. https://doi.org/10.1111/ajgw.12010

Buch-Pedersen, M. J., Rudashevskaya, E. L., Berner, T. S., Venema, K., & Palmgren, M. G. (2006). Potassium as an intrinsic uncoupler of the plasma membrane H^+-ATPase. *Journal of Biological Chemistry*, *281*(50), 38285-38292. https://doi.org/10.1074/jbc.M604781200

Cameron, W., Petrie, P. R., Barlow, E. W. R., Patrick, C. J., Howell, K., & Fuentes, S. (2020). Advancement of grape maturity: comparison between contrasting cultivars and regions. *Australian Journal of Grape and Wine Research*, *26*(1), 53-67. https://doi.org/10.1111/ajgw.12414

Carlomagno, A., Novello, V., Ferrandino, A., Genre, A., Lovisolo, C., & Hunter, J. J. (2018). Pre-harvest berry shrinkage in cv 'Shiraz' (*Vitis vinifera* L.): understanding sap flow by means of tracing. *Scientia Horticulturae*, *233*, 394-406. https://doi.org/10.1016/j.scienta.2018.02.014

Chen, M. Y., Lin, H. T., Zhang, S., Lin, Y. F., Chen, Y. H., & Lin, Y. X. (2015). Effects of adenosine triphosphate (ATP) treatment on postharvest physiology, quality and storage behavior of longan fruit. *Food and Bioprocess Technology*, *8*, 971-982. https://doi.org/10.1007/s11947-014-1462-z

Clark, G., & Roux, S. J. (2018). Role of Ca^{2+} in mediating plant responses to extracellular ATP and ADP. *International Journal of Molecular Sciences*, *19*(11), Article 3590. https://doi.org/10.3390/ijms19113590

Clarke, S. J., & Rogiers, S. Y. (2019). The role of fruit exposure in the late season decline of grape berry mesocarp cell vitality. *Plant Physiology and Biochemistry*, *135*, 69-76. https://doi.org/10.1016/j.plaphy.2018.11.025

Coetzee, Z. A., Walker, R. R., Deloire, A. J., Barril, C., Clarke, S. J., & Rogiers, S. Y. (2017). Impact of reduced atmospheric CO_2 and varied potassium supply on carbohydrate and potassium distribution in grapevine and grape berries (*Vitis vinifera* L.). *Plant Physiology and Biochemistry*, *120*, 252-260. https://doi.org/10.1016/j.plaphy.2017.10.008

Coetzee, Z. A., Walker, R. R., Liao, S., Barril, C., Deloire, A. J., Clarke, S. J., Tyerman, S. D., & Rogiers, S. Y. (2019). Expression patterns of genes encoding sugar and potassium transport proteins are simultaneously upregulated or downregulated when carbon and potassium availability is modified in Shiraz (*Vitis vinifera* L.) berries. *Plant & Cell Physiology*, *60*(10), 2331-2342. https://doi.org/10.1093/pcp/pcz130

Coombe, B. G. (1976). The development of fleshy fruits. *Annual Review of Plant Physiology*, *27*(1), 207-228. https://doi.org/10.1146/annurev.pp.27.060176.001231

Coombe, B. G. (1995). Growth Stages of the Grapevine: Adoption of a system for identifying grapevine growth stages. *Australian Journal of Grape and Wine Research*, *1*(2), 104-110. https://doi.org/10.1111/j.1755-0238.1995.tb00086.x

Cui, J., & Tcherkez, G. (2021). Potassium dependency of enzymes in plant primary metabolism. *Plant Physiology and Biochemistry*, *166*, 522-530. https://doi.org/10.1016/j.plaphy.2021.06.017

Demidchik, V. (2018). ROS-activated ion channels in plants: biophysical characteristics, physiological functions and molecular nature. *International Journal of Molecular Sciences*, *19*(4), Article 1263. https://doi.org/10.3390/ijms19041263

Demidchik, V., & Shabala, S. (2018). Mechanisms of cytosolic calcium elevation in plants: the role of ion channels, calcium extrusion systems and NADPH oxidase-mediated 'ROS-Ca^{2+} Hub'. *Functional Plant Biology*, *45*(2), 9-27. https://doi.org/10.1071/FP16420

Famiani, F., Farinelli, D., Palliotti, A., Moscatello, S., Battistelli, A., & Walker, R. P. (2014). Is stored malate the quantitatively most important substrate utilised by respiration and ethanolic fermentation in grape berry pericarp during ripening? *Plant Physiology and Biochemistry*, *76*, 52-57. https://doi.org/10.1016/j.plaphy.2013.12.017

Fuentes, S., Sullivan, W., Tilbrook, J., & Tyerman, S. (2010). A novel analysis of grapevine berry tissue demonstrates a variety-dependent correlation between tissue vitality and berry shrivel. *Australian Journal of Grape and Wine Research*, *16*(2), 327-336. https://doi.org/10.1111/j.1755-0238.2010.00095.x

Gajdanowicz, P., Michard, E., Sandmann, M., Rocha, M., Corrêa, L. G. G., Ramirez-Aguilar, S. J., Gomez-Porras, J. L., González, W., Thibaud, J. B., van Dongen, J. T., & Dreyer, I. (2011). Potassium (K^+) gradients serve as a mobile energy source in plant vascular tissues. *Proceedings of the National Academy of Sciences of the United States of America*, *108*(2), 864-869. https://doi.org/10.1073/pnas.1009777108

Greer, D. H., & Rogiers, S. Y. (2009). Water flux of *Vitis vinifera* L. cv. Shiraz bunches throughout development and in relation to late-season weight loss. *American Journal of Enology and Viticulture*, *60*(2), 155-163. https://doi.org/10.5344/ajev.2009.60.2.155

Hanana, M., Cagnac, O., Yamaguchi, T., Hamdi, S., Ghorbel, A., & Blumwald, E. (2007). A grape berry (*Vitis vinifera* L.) cation/proton antiporter is associated with berry ripening. *Plant & Cell Physiology*, *48*(6), 804-811. https://doi.org/10.1093/pcp/pcm048

Hou, Q. Z., Wang, Y. P., Fan, B. Q., Sun, K., Liang, J. Y., Feng, H. Q., & Jia, L. Y. (2020). Extracellular ATP affects cell viability, respiratory O_2 uptake, and intracellular ATP production of tobacco cell suspension culture in response to hydrogen peroxide-induced oxidative stress. *Biologia*, *75*(9), 1437-1443. https://doi.org/10.2478/s11756-020-00442-w

Igamberdiev, A. U., & Kleczkowski, L. A. (2001). Implications of adenylate kinase-governed equilibrium of adenylates on contents of free magnesium in plant cells and compartments. *Biochemical Journal*, *360*(1), 225-231. https://doi.org/10.1042/bj3600225

Igamberdiev, A. U., & Kleczkowski, L. A. (2011). Magnesium and cell energetics in plants under anoxia. *Biochemical Journal*, *437*, 373-379. https://doi.org/10.1042/BJ20110213

Igamberdiev, A. U., & Kleczkowski, L. A. (2021). Pyrophosphate as an alternative energy currency in plants. *Biochemical Journal*, *478*(8), 1515-1524. https://doi.org/10.1042/BCJ20200940

Jarvis, C., Barlow, E., Darbyshire, R., Eckard, R., & Goodwin, I. (2017). Relationship between viticultural climatic indices and grape maturity in Australia. *International Journal of Biometeorology*, *61*(10), 1849-1862. https://doi.org/10.1007/s00484-017-1370-9

Jeschke, W. D., Wolf, O., & Hartung, W. (1992). Effect of NaCI salinity on flows and partitioning of C, N, and mineral ions in whole plants of white lupin, *Lupinus albus* L. *Journal of Experimental Botany*, *43*(251), 777-788. https://doi.org/10.1093/jxb/43.6.777

Köpnick, C., Grübe, M., Stock, J., Senula, A., Mock, H. P., & Nagel, M. (2018). Changes of soluble sugars and ATP content during DMSO droplet freezing and PVS3 droplet vitrification of potato shoot tips. *Cryobiology*, *85*, 79-86. https://doi.org/10.1016/j.cryobiol.2018.09.005

Kuang, L. Q., Chen, S. W., Guo, Y., & Ma, H. Q. (2019). Quantitative proteome analysis reveals changes in the protein landscape during grape berry development with a focus on vacuolar transport proteins. *Frontiers in Plant Science*, *10*, Article 641. https://doi.org/10.3389/fpls.2019.00641

Maathuis, F. J. M., & Amtmann, A. (1999). K^+ nutrition and Na^+ toxicity: the basis of cellular K^+/Na^+ ratios. *Annals of Botany*, *84*(2), 123-133. https://doi.org/10.1006/anbo.1999.0912

Maathuis, F. J. M. (2014). Sodium in plants: perception, signalling, and regulation of sodium fluxes. *Journal of Experimental Botany*, *65*(3), 849-858. https://doi.org/10.1093/jxb/ert326

Munns, R. (2002). Comparative physiology of salt and water stress. *Plant, Cell & Environment*, *25*(2), 239-250. https://doi.org/10.1046/j.0016-8025.2001.00808.x

Oria-Hernández, J., Cabrera, N., Pérez-Montfort, R., & Ramírez-Silva, L. (2005). Pyruvate kinase revisited: the activating effect of K^+. *Journal of Biological Chemistry*, *280*(45), 37924-37929. https://doi.org/10.1074/jbc.M508490200

Prathap, V., Kumar, A., Maheshwari, C., & Tyagi, A. (2022). Phosphorus homeostasis: acquisition, sensing, and long-distance signaling in plants. *Molecular Biology Reports*, *49*(8), 8071-8086. https://doi.org/10.1007/s11033-022-07354-9

Rogiers, S. Y., Greer, D. H., Hatfield, J. M., Orchard, B. A., & Keller, M. (2006a). Solute transport into Shiraz berries during development and late-ripening shrinkage. *American Journal of Enology and Viticulture*, *57*(1), 73-80. https://doi.org/10.5344/ajev.2006.57.1.73

Rogiers, S. Y., Greer, D. H., Hatfield, J. M., Orchard, B. A., & Keller, M. (2006b). Mineral sinks within ripening grape berries (*Vitis vinifera* L.). *VITIS - Journal of Grapevine Research*, *45*(3), 115-123. https://ojs.openagrar.de/index.php/VITIS/article/view/4282/4234

Rogiers, S. Y., & Holzapfel, B. P. (2015). The plasticity of berry shrivelling in 'Shiraz': a vineyard survey. *VITIS - Journal of Grapevine Research*, *54*(1), 1-8. https://doi.org/10.5073/vitis.2015.54.1-8

Rogiers, S. Y., Coetzee, Z. A., Walker, R. R., Deloire, A., & Tyerman, S. D. (2017). Potassium in the grape (*Vitis vinifera* L.) berry: transport and function. *Frontiers in Plant Science*, *8*, Article 1629. https://doi.org/10.3389/fpls.2017.01629

Salinas, R., Sánchez, E., Ruíz, J. M., Lao, M. T., & Romero, L. (2013). Phosphorus levels influence plasma membrane H^+-ATPase activity and K^+, Ca^{2+}, and Mg^{2+} assimilation in green bean. *Communications in Soil Science and Plant Analysis*, *44*(1-4), 456-464. https://doi.org/10.1080/00103624.2013.744127

Saquet, A. A., Streif, J., & Bangerth, F. (2000). Changes in ATP, ADP and pyridine nucleotide levels related to the incidence of physiological disorders in 'Conference' pears and 'Jonagold' apples during controlled atmosphere storage. *The Journal of Horticultural Science and Biotechnology*, *75*(2), 243-249. https://doi.org/10.1080/14620316.2000.11511231

Saquet, A. A., Streif, J., & Bangerth, F. (2003). Energy metabolism and membrane lipid alterations in relation to brown heart development in 'Conference' pears during delayed controlled atmosphere storage. *Postharvest Biology and Technology*, *30*(2), 123-132. https://doi.org/10.1016/S0925-5214(03)00099-1

Savoi, S., Torregrosa, L., & Romieu, C. (2021). Transcripts switched off at the stop of phloem unloading highlight the energy efficiency of sugar import in the ripening *V. vinifera* fruit. *Horticulture Research*, *8*(1), Article 193. https://doi.org/10.1038/s41438-021-00628-6

Shabala, S., & Wilson, S. (2001). Fluctuations in light intensity modulate ion fluxes from grape berry mesocarp: direct evidence from microelectrode ion flux estimations. *Australian Journal of Grape and Wine Research*, *7*(3), 137-143. https://doi.org/10.1111/j.1755-0238.2001.tb00201.x

Smyth, D. A., & Black, C. C. (1984). Measurement of the pyrophosphate content of plant tissues. *Plant Physiology*, *75*(3), 862-864. https://doi.org/10.1104/pp.75.3.862

Sun, J., Zhang, C. L., Deng, S. R., Lu, C. F., Shen, X., Zhou, X. Y., Zheng, X. J., Hu, Z. M., & Chen, S. L. (2012). An ATP signalling pathway in plant cells: extracellular ATP triggers programmed cell death in *Populus euphratica*. *Plant, Cell & Environment*, *35*(5), 893-916. https://doi.org/10.1111/j.1365-3040.2011.02461.x

Terrier, N., Issaly, N., Sauvage, F. X., Ageorges, A., & Romieu, C. (1997). Aspects of grape berry development bioenergetics.*Acta Horticulturae* [Proceedings of the fifth international symposium on grapevine physiology]. ISHS Acta Horticulturae 526: V International Symposium on Grapevine Physiology,

Terrier, N., Deguilloux, C., Sauvage, F. X., Martinoia, E., & Romieu, C. (1998). Proton pumps and anion transport in *Vitis vinifera*: The inorganic pyrophosphatase plays a predominant role in the energization of the tonoplast. *Plant Physiology and Biochemistry*, *36*(5), 367-377. https://doi.org/10.1016/S0981-9428(98)80078-8

Terrier, N., Sauvage, F.-X., Ageorges, A., & Romieu, C. (2001). Changes in acidity and in proton transport at the tonoplast of grape berries during development. *Planta*, *213*(1), 20-28. https://doi.org/10.1007/s004250000472

Tilbrook, J., & Tyerman, S. D. (2008). Cell death in grape berries: varietal differences linked to xylem pressure and berry weight loss. *Functional Plant Biology*, *35*(3), 173-184. https://doi.org/10.1071/FP07278

Tilbrook, J., & Tyerman, S. D. (2009). Hydraulic connection of grape berries to the vine: varietal differences in water conductance into and out of berries, and potential for backflow. *Functional Plant Biology*, *36*(6), 541-550. https://doi.org/10.1071/FP09019

Tyerman, S. D., Tilbrook, J., Pardo, C., Kotula, L., Sullivan, W., & Steudle, E. (2004). Direct measurement of hydraulic properties in developing berries of *Vitis vinifera* L. cv Shiraz and Chardonnay. *Australian Journal of Grape and Wine Research*, *10*(3), 170-181. https://doi.org/10.1111/j.1755-0238.2004.tb00020.x

Wang, H., An, T. T., Huang, D., Liu, R. J., Xu, B. C., Zhang, S. Q., Deng, X. P., Siddique, K. H. M., & Chen, Y. L. (2021). Arbuscular mycorrhizal symbioses alleviating salt stress in maize is associated with a decline in root-to-leaf gradient of Na^+/K^+ ratio. *BMC Plant Biology*, *21*, Article 457. https://doi.org/10.1186/s12870-021-03237-6

Webb, L. B., Whetton, P. H., Bhend, J., Darbyshire, R., Briggs, P. R., & Barlow, E. W. R. (2012). Earlier wine-grape ripening driven by climatic warming and drying and management practices. *Nature Climate Change*, *2*(4), 259-264. https://doi.org/10.1038/nclimate1417

Xiao, Z., Liao, S., Rogiers, S. Y., Sadras, V. O., & Tyerman, S. D. (2018a). Effect of water stress and elevated temperature on hypoxia and cell death in the mesocarp of Shiraz berries. *Australian Journal of Grape and Wine Research*, *24*(4), 487-497. https://doi.org/https://doi.org/10.1111/ajgw.12363

Xiao, Z., Rogiers, S. Y., Sadras, V. O., & Tyerman, S. D. (2018b). Hypoxia in grape berries: the role of seed respiration and lenticels on the berry pedicel and the possible link to cell death. *Journal of Experimental Botany*, *69*(8), 2071-2083. https://doi.org/10.1093/jxb/ery039

Xiao, Z. Y., Chin, S., White, R. G., Gourieroux, A. M., Pagay, V., Tyerman, S. D., Schmidtke, L. M., & Rogiers, S. Y. (2021). Vascular connections into the grape berry: the link of structural investment to seededness. *Frontiers in Plant Science*, *12*, Article 662433. https://doi.org/10.3389/fpls.2021.662433

Zhang, X. Y., Wang, X. L., Wang, X. F., Xia, G. H., Pan, Q. H., Fan, R. C., Wu, F. Q., Yu, X. C., & Zhang, D. P. (2006). A shift of phloem unloading from symplasmic to apoplasmic pathway is involved in developmental onset of ripening in grape berry. *Plant Physiology*, *142*(1), 220-232. https://doi.org/10.1104/pp.106.081430

Zhang, Y., & Keller, M. (2017). Discharge of surplus phloem water may be required for normal grape ripening. *Journal of Experimental Botany*, *68*(3), 583-593. https://doi.org/10.1093/jxb/erw476